

REAL-TIME ACID TREATMENT PERFORMANCE ANALYSIS OF GEOTHERMAL WELLS

Frederick Libert¹, Peter¹, Riza Pasikki¹, Keita Yoshioka², and Mark Looney²

1. Chevron Geothermal Salak, Jakarta 10270, Indonesia
2. Chevron Energy Technology Company, Houston TX 77002, USA
e-mail: yoshk@chevron.com

ABSTRACT

In the Salak geothermal field, a five well acid treatment campaign was conducted in 2008. The choice of candidate wells for stimulation was based on low production/injection capacity, flowing wellhead pressure below normal system operating pressure, and massive water-based mud losses while drilling the reservoir section. After the wells were selected, the treatments were designed as follows: 1) select the target intervals, 2) select the acids and additives for pre- and post-flush stages, and (3) identify the acid concentrations and volumes.

The performance of the acid treatments and the adequacy of the treatment design are conventionally evaluated by measuring injectivity before and after stimulation. Through this process, we can obtain quantitative evaluation of the treatment. However, with the existing practices we cannot assess on-site the change of well characteristics as result of acid stimulation.

In this study we applied real-time acid treatment performance analysis tools, which have proved to be effective in oil and gas reservoirs, to a geothermal reservoir, the Salak Field in West Java. We evaluated these methods to monitor time variant skin factor and/or injectivity change in the course of acid stimulation. The field data clearly depict skin factor evolution over time. By tracking the real-time performance, improvements for future acid treatment design were identified.

INTRODUCTION

An infill drilling program has been implemented at Salak since 2006. Several new steam production wells drilled during this campaign show low production performances. Well #1 and Well #2 were two wells drilled in 2006 – 2007 that could not deliver steam at system operating pressures. Drilling

records and well test analysis suggest that they experienced formation damage from invasion of drilling cuttings and water-based mud. An acid stimulation campaign was carried out in October - November 2008 to improve their production. Acid treatment in Salak is found to be a very effective means to increase well's productivity or injectivity (Mahajan *et al.*, 2006; Pasikki and Gilmore, 2006). Six acid stimulations performed in the Salak between 2004 – 2007 have successfully improved production characteristics of the wells with evidence of formation damage. The average productivity index (PI) improvement from acid job is 200%.

In the 2008 acid stimulation campaign, a commercial acid system was used that consisted of 15% wt. HCl for pre-flush and 9% wt. HF for the main flush. A two-inch coiled tubing was reciprocated across the targeted interval to place the acids.

REAL TIME ACID TREATMENT ANALYSIS

Several real-time evaluation methods of acid treatment from the pressure response and rate measurements are available in oil and gas reservoirs and they are successfully deployed. These methods enable engineers to monitor the stimulation performance on-site (Montgomery *et al.*, 1995; Al-Dhafeeri *et al.*, 2002), and also design a treatment with optimal use of acid volume for each stage (Boonyapaluk and Hareland, 1996).

Real-time analysis was first introduced by Paccaloni (1979). In the method, he assumed a steady-state radial flow inside the acid bank and the pressure response can be expressed from Darcy's law as:

$$p_{wf} - p_r = \frac{141.2qB\mu}{kh} \left(\ln \frac{r_b}{r_w} + s \right), \quad (1)$$

where r_b is the acid bank radius.

From Eq. 1, the time variant skin factor can be computed as:

$$s(t) = \frac{0.00708 kh(p_{wf}(t) - p_r)}{Bq(t)\mu} - \ln \frac{r_b}{r_w}. \quad (2)$$

Using Eq. 2, we can update the skin factor with the real-time monitored pressure response, p_{wf} and injection rate, q . As for the acid bank radius, r_b , the value of 3 to 4 ft is suggested. The proposed method has been widely applied in many fields and found to be an effective tool in inferring skin factor evolution during the treatment. However, the assumption of steady-state may mask the transition effects, which are expected to take place over the treatment considering a rather short duration of injection.

Prouvost and Economides (1989) proposed a real-time acidizing evaluation method taking account of transient effects. Skin factor is defined as a dimensionless pressure difference between ideal condition and real situation. Letting a simulated pressure be ideal, we can calculate time variant skin factor as:

$$s(t) = s_o + \frac{0.00708 kh}{q(t)B(t)\mu(t)} [p_{meas}(t) - p_{sim}(t, s_o)]. \quad (3)$$

where p_{meas} , p_{sim} , and s_o are the measured and simulated pressures, and the original skin factor respectively.

If we assume single phase fluid injection into a cylindrical formation with the initial pressure p_i , we can apply line source solution to Eq. 3 (Heard *et al.*, 1990). Then we have:

$$p_{sim} = p_i + \frac{162.6qB\mu}{kh} \left[\log t + \log \left(\frac{k}{\phi\mu c_t r_w^2} \right) - 3.23 + 0.87s_o \right] \quad (4)$$

Substituting Eq.4 into Eq. 3, we obtain:

$$s(t) = \frac{kh}{141.2B\mu} \left(\frac{p_{meas}(t) - p_i}{q(t)} \right) - \frac{\log t_D}{0.87}, \quad (5)$$

where t_D is:

$$t_D = 0.000264 kt / \phi\mu c_t r_w^2. \quad (6)$$

Since we assume reservoir parameters are constant, time variant skin can be calculated from Eq. 5 by using the pressure response and injection rate record.

Zhu and Hill (1998) also applied line source solution to real-time skin factor analysis and furthermore they took into consideration the multiple rate changes during acid treatment. The pressure transient response to multi-rate injection is given as (Earlougher, 1977):

$$\frac{p_i - p_{wf}}{q_N} = m\Delta t_{sup} + b, \quad (7)$$

Where:

$$m = \frac{162.6B\mu}{kh}, \quad (8)$$

$$b = m \left[\log \left(\frac{k}{\phi\mu c_t r_w^2} \right) - 3.23 + 0.87s \right], \quad (9)$$

and

$$\Delta t_{sup} = \sum_{j=1}^N \left(\frac{q_j - q_{j-1}}{q_N} \right) \log(t_N - t_{j-1}). \quad (10)$$

Assuming that skin factor is the only variable during acid treatment, we can find b as the intercept on the plot of inverse injectivity $(p_i - p_{wf})/q_N$, vs. the superposition time Δt_{sup} . Since the slope of this straight line, m is assumed to be invariant, skin evolution can be computed as:

$$s = \frac{1}{0.87} \left[\frac{b}{m} - \log \left(\frac{k}{\phi\mu c_t r_w^2} \right) + 3.23 \right]. \quad (11)$$

Then we update b from Eq. 4 as:

$$b = \frac{p_i - p_{wf}}{q_N} - m\Delta t_{sup}. \quad (12)$$

By applying the superposition time, we can remove the skin effects from the rate changes and trace the skin effect as flow restrictions or enhancements.

ANALYSIS METHOD COMPARISON

We have introduced three different acid treatment analysis methods widely applied in oil and gas

industry. In this section, we compare the methods with acid treatment data recorded from geothermal wells in Salak field, Indonesia.

In applying the methods described above, we assume:

- Each feed zone acts as a separated layer.
- All the injection volume go into the targeted feed zone as we aimed.
- Single phase radial flow.

Considering that each feed zones are separated by distances of 50 –1500 ft, the first assumption should be reasonable. From post-acid job spinner surveys, we are aware that some portion of the acid is taken at different depths and some zones are stimulated unintentionally. Although this reallocation of acid may deceive the estimation of skin factor value itself at the targeted zone, the relative skin change from the initial condition should stand out. In the third assumption, we neglect fluid properties difference between acid and reservoir fluid (water), and spatial reservoir parameter variation. These details can be accounted for by applying numerical simulation. However, given the uncertainties in reservoir characterizations and complications in non-newtonian rheology, the rewards we gain from numerical simulation may be limited. Instead, we apply a simple analytical approach for an inexpensive and comprehensive real-time analysis. We also emphasize that the skin factor obtained from these methods includes not only mechanical (formation damage) but also fluid bank effect (viscosity changes), and geometrical skin (deviation from radial), etc.

Tables 1 and 2 show acid treatment data recorded during treatment of Well #1 (MD 6250 – 6370 ft) and Well #2 zone I (MD 5330 – 5410 ft). Injection rates are recorded at coiled tubing and annulus, and the pressure response is recorded at the tubing head. Therefore, the bottomhole pressure needs to be calculated from the tubing pressure. The bottomhole pressure estimation procedure is discussed in Appendix A. Real-time analysis results from three different methods are compared in Figs 1 and 2. The reservoir and coiled tubing parameters used in the analysis are listed in Tables 3 and 4.

Time (min)	q -CT (bpm)	q -AN (bpm)	Pti (psi)	Fluid
2	5.09	4.91	1361.69	Pre-flush
4	5.08	5.04	1345.08	Pre-flush
6	5.07	5.56	1338.08	Pre-flush
8	5.07	5.53	1335.67	Pre-flush
10	5.08	5.36	1332.75	Pre-flush
12	5.08	5.09	1331.92	Pre-flush
14	5.08	5.03	1326.33	Pre-flush
16	5.07	5.11	1329.75	Pre-flush
18	5.06	5.13	1370.58	Pre-flush
20	5.08	5.16	1372.75	Pre-flush
22	5.08	5.15	1366.42	Pre-flush
24	5.07	5.04	1373.08	Pre-flush
26	5.07	4.98	1382.83	Pre-flush
28	5.06	4.97	1389.67	Pre-flush
30	5.06	4.93	1403.33	Pre-flush
32	5.06	4.96	1414.25	Pre-flush
34	5.06	4.91	1415.33	Pre-flush
36	5.06	4.92	1423.42	Pre-flush
38	5.06	5.00	1416.00	Pre-flush
40	5.06	5.05	1371.75	Pre-flush
42	5.06	5.14	1368.58	Pre-flush
44	5.06	5.18	1364.00	Pre-flush
46	5.06	5.21	1356.75	Pre-flush
48	5.07	5.21	1358.33	Pre-flush
50	5.08	5.19	1354.50	Pre-flush
52	5.08	5.13	1349.50	Pre-flush
54	5.08	5.12	1341.17	Pre-flush
56	5.08	5.05	1339.00	Main-flush
58	5.08	5.06	1338.58	Main-flush
60	5.10	5.04	1262.75	Main-flush
62	5.09	5.05	1215.92	Main-flush
64	5.08	5.04	1226.08	Main-flush
66	5.08	5.03	1241.92	Main-flush
68	5.08	5.02	1240.58	Main-flush
70	5.07	5.03	1246.25	Main-flush
72	5.09	5.07	1254.67	Main-flush
74	5.04	5.06	1245.25	Main-flush
76	5.01	5.05	1303.08	Main-flush
78	4.97	5.00	1492.08	Main-flush
80	5.02	5.01	1288.50	Main-flush
82	5.03	5.03	1277.50	Main-flush
84	5.03	5.05	1275.75	Main-flush
86	5.03	5.05	1277.50	Main-flush
88	5.02	5.03	1280.25	Main-flush
90	5.02	4.99	1273.33	Main-flush
92	5.04	4.99	1278.92	Main-flush
94	5.05	5.00	1275.00	Main-flush
96	5.05	4.99	1277.17	Main-flush
98	5.04	5.01	1267.33	Main-flush
100	5.05	4.98	1211.17	Main-flush
102	5.04	5.00	1216.50	Main-flush
104	5.03	5.00	1247.25	Main-flush
106	5.02	4.96	1280.17	Main-flush
108	5.03	4.99	1271.17	Main-flush
110	5.03	5.04	1263.67	Main-flush
112	5.04	5.00	1257.00	Main-flush
114	5.03	5.01	1260.25	Main-flush
116	5.02	5.12	1345.33	Main-flush
118	4.97	5.12	1678.75	Main-flush
121	4.99	5.08	1593.67	Main-flush
126	4.05	5.01	1925.13	Water
131	3.53	5.01	2132.90	Water
136	3.52	5.02	2200.37	Water
141	3.55	5.04	1841.27	Water
146	3.55	7.75	1568.97	Water
151	3.51	10.30	2139.83	Water
156	3.52	8.08	2187.07	Water
161	3.52	8.14	2191.93	Water
166	3.50	10.05	2166.03	Water
171	3.50	10.08	2160.19	Water

Table 1. Treatment record from Well#1.

Time (min)	q -CT (bpm)	q -AN (bpm)	Pti (psi)	Fluid
2.5	5.13	5.01	1554.53	Pre-flush
5.0	5.08	5.01	1523.08	Pre-flush
7.5	4.89	5.01	1431.62	Pre-flush
10.0	5.01	5.01	1473.05	Pre-flush
12.5	5.13	5.01	1547.25	Pre-flush
15.0	5.09	5.01	1545.81	Pre-flush
17.5	5.13	5.01	1549.34	Main-flush
20.0	5.13	5.01	1528.89	Main-flush
22.5	5.13	5.01	1519.43	Main-flush
25.0	5.13	5.01	1496.98	Main-flush
27.5	5.14	5.01	1502.31	Main-flush
30.0	5.15	5.01	1509.29	Main-flush
32.5	5.15	5.01	1525.92	Main-flush
35.0	5.11	5.01	1535.34	Main-flush
37.5	5.12	5.01	1535.63	Main-flush
40.0	5.13	5.01	1515.14	Main-flush
42.5	3.08	5.01	608.39	Main-flush
45.0	2.86	5.01	671.78	Main-flush
47.5	3.97	5.01	1042.22	Main-flush
50.0	4.98	5.01	1453.15	Main-flush
52.5	4.98	5.01	1432.70	Main-flush
55.0	4.99	5.01	1427.64	Main-flush
57.5	5.03	5.01	1405.14	Main-flush
60.0	5.11	5.01	1315.65	Main-flush
62.5	5.14	5.01	1384.41	Main-flush
65.0	5.02	5.01	1330.32	Main-flush
67.5	4.82	5.01	1331.62	Main-flush
70.0	4.86	16.03	1976.00	Water
72.5	4.51	16.03	3024.00	Water
75.0	3.77	16.03	2763.00	Water
77.5	3.6	16.03	2498.00	Water
80.0	3.58	16.03	2486.00	Water
82.5	3.57	16.03	2456.00	Water
85.0	3.56	16.03	2447.00	Water
87.5	3.57	16.03	2449.00	Water
90.0	3.57	16.03	2485.00	Water
92.5	3.1	16.03	1710.00	Water

Table 2. Treatment record from Well#2 zone I.

Reservoir/Fluid		Coiled Tubing/Wellbore	
Pr [psi]	1165	rw [ft]	1
B	1	Tubing [in]	2.1
Φ	0.1	ϵ	0.00001
Ct [1/psij]	0.000003	L [ft]	10500
h [ft]	100	ρ [lbm/ft ³]	68
k [md]	20	Sp	1.1
μ [cp]	0.5	Z	6300

Table 3. Parameters for Well#1 analysis.

Reservoir/Fluid		Coiled Tubing/Wellbore	
Pr [psi]	1050	rw [ft]	1
B	1	Tubing [in]	2.1
Φ	0.1	ϵ	0.00001
Ct [1/psij]	0.000003	L [ft]	10500
h [ft]	100	ρ [lbm/ft ³]	68
k [md]	30	Sp	1.1
μ [cp]	0.5	Z	5400

Table 4. Parameters for Well#2 zone I analysis.

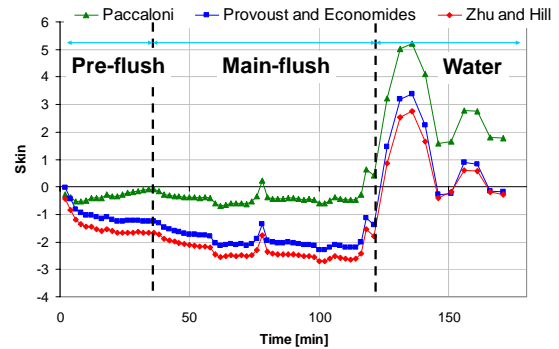


Figure 1 Comparison results for Well#1.

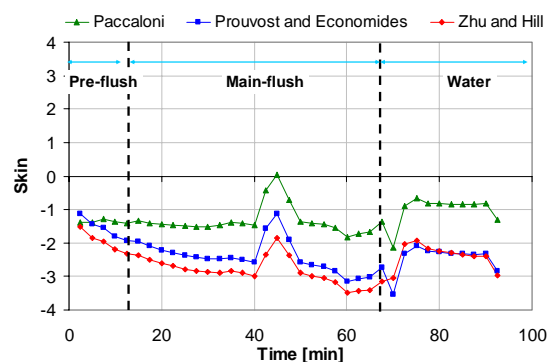


Figure 2 Comparison results for Well#2.

A pre-acid stimulation survey of Well #1 shows that the injectivity index (II) increases from 4.3 kph/psi to 5.1 kph/psi. However, this much change is in general considered to be very nominal in pressure-temperature-spinner (PTS) surveys. Thus we conclude that Well #1 did not improve from the treatment. In figure 1, higher skin factor than that of initial is indicated by all three methods. While the Prouvost and Economides, and Zhu and Hill methods generate quite similar skin factor responses, Paccaloni's method overestimates skin factor in most periods and ends up with a much higher overall value. Also both the Prouvost and Economides, and Zhu and Hill methods indicate some skin factor improvements during pre-flush and main acid flow periods but Paccaloni's method does not depict skin decrease over the acid flowing period.

The injectivity of Well #2 after treating three zones increases from 6.6 kph/psi to 31.2 kph/psi. The acid treatment is currently considered as a great success. Unfortunately, a post-treatment spinner survey is not available yet. Therefore, we are uncertain about the improvements of each zone. In figure 2, both the Prouvost and Economides, and Zhu and Hill methods show a decreasing trend in skin factor during the acidizing. They show a skin increase during water

flush but the skin becomes small again at the end. However, Paccaloni's method again indicates higher skin values than the other two methods and estimates almost the same final skin. Considering the injectivity improvement in this well, the analysis by Paccaloni's method is contradictory.

Although our main purpose is not a quantification of skin evolution but rather a qualitative analysis, it is obvious from the comparison results shown above that Paccaloni's method is not successful in detecting skin improvement during pre-flush and main acid treatment period. We can also note that the Prouvost and Economides, and Zhu and Hill methods generate very similar analysis results. Both methods consider transient effects. Since Zhu and Hill's method takes into account multi-rate effects, their method will be used in the rest of treatment analysis in this study.

SENSITIVITY TO UNCERTAINTIES

We have conducted a real-time skin factor monitoring analysis for two acid treatments and the results correspond to the injectivity data recorded before and after the stimulation in both analyses. However, the reservoir parameters used in the analyses are uncertain to us because it is not common to measure the permeability-thickness product, kh , for each feeding zone. In addition, the viscosity, μ is highly affected by temperature, and the amount of dissolved minerals. Therefore, we have to confront the uncertainties in these parameters in real-time skin analysis. In this section, we infer the sensitivity of skin factor to those uncertainties.

We grouped the permeability-thickness product, kh and viscosity μ into one term, kh/μ and conducted an analysis by changing its value. Figure 3 shows skin factor evolution with different kh/μ terms.

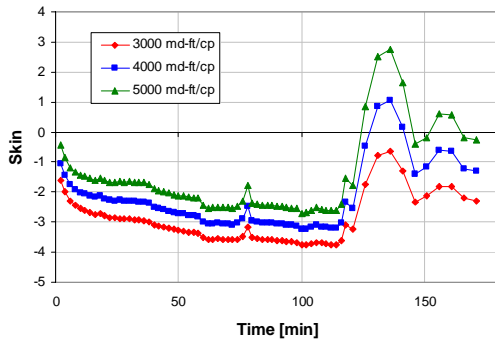


Figure 3 Skin factor sensitivity to kh/μ - Well#1.

Skin factor evolutions show similar trends during the acidizing period and differ in the water flush period. Next we defined the injectivity index, I as:

$$I = \frac{0.000103kh}{\mu[\ln(r_e/r_w) + s]} \quad (13)$$

This injectivity index will change with the time variant skin. Then we normalized the injectivity index to the initial injectivity. Figure 4 plots the evolution of the normalized injectivity.

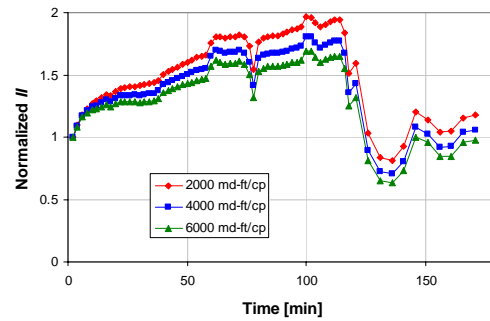


Figure 4 Normalized injectivity index sensitivity to kh/μ - Well#1

In all our analyses, the overall injectivity index shows a small decrease or increase, which supports the field observation. More importantly, general trends for injectivity appear to be similar. All scenarios indicate injectivity improvement during pre-flush and main acid and impairment during the water flush.

A similar sensitivity study was conducted on Well #2 zone I (MD 5330 – 5410 ft) and zone III (MD 5920 – 6170 ft). The treatment data from Well #2 zone III are shown in Table 5. The analysis of zone II is not included since we misplaced the feeding zone. Figures 5 and 6 show skin factor evolution sensitivities to kh/μ .

Time (min)	q-CT (bpm)	q-AN (bpm)	Pti (psi)	Fluid
5.01	5.12	5.02	1432.06	Pre-flush
7.50	5.11	5.02	1426.74	Pre-flush
10.01	5.11	5.02	1417.03	Pre-flush
12.50	5.10	5.02	1407.72	Pre-flush
17.51	5.12	5.02	1386.69	Pre-flush
20.02	5.12	5.02	1340.99	Pre-flush
22.51	5.08	5.02	1323.67	Pre-flush
25.02	5.08	5.02	1316.96	Pre-flush
30.02	5.12	5.02	1308.94	Pre-flush
32.52	5.07	5.02	1291.23	Pre-flush
37.52	5.08	5.02	1282.21	Pre-flush
40.03	5.09	5.02	1268.50	Pre-flush
42.52	5.14	5.02	1287.18	Pre-flush
45.02	5.12	5.02	1136.47	Pre-flush
50.02	5.10	5.02	1223.45	Pre-flush
52.53	5.10	5.02	1209.13	Pre-flush
57.53	5.13	5.02	1253.86	Pre-flush
65.03	5.08	5.02	1244.90	Pre-flush
67.53	5.04	5.02	1260.69	Pre-flush
70.04	5.10	5.02	1276.02	Pre-flush
77.54	5.07	5.02	1259.10	Pre-flush
80.03	5.06	5.02	1262.78	Pre-flush
85.05	5.13	5.02	1262.50	Pre-flush
90.04	5.11	5.02	1248.83	Main-flush
97.55	5.05	5.02	1341.92	Main-flush
100.04	5.06	5.02	1334.43	Main-flush
102.56	5.05	5.02	1326.33	Main-flush
110.05	5.06	5.02	1303.46	Main-flush
112.56	5.06	5.02	1285.57	Main-flush
115.05	5.06	5.02	1292.08	Main-flush
120.06	5.17	5.02	1183.31	Main-flush
122.57	5.17	5.02	1183.66	Main-flush
125.06	5.14	5.02	1182.30	Main-flush
130.07	4.98	5.02	1162.56	Main-flush
132.56	5.02	5.02	1182.19	Main-flush
135.07	5.02	5.02	1205.22	Main-flush
142.58	5.17	5.02	1351.90	Main-flush
147.57	4.93	5.02	1290.51	Main-flush
150.08	5.06	5.02	1346.48	Main-flush
157.58	5.08	5.02	1314.50	Main-flush
160.08	5.06	5.02	1287.05	Main-flush
162.58	5.04	5.02	1328.99	Main-flush
170.08	5.04	5.02	1193.01	Main-flush
172.58	5.11	5.02	1205.95	Main-flush
177.58	5.10	5.02	1180.43	Main-flush
182.58	5.10	5.02	1150.92	Main-flush
187.59	5.03	5.02	1592.12	Main-flush
190.10	5.04	5.02	1312.97	Main-flush
197.59	5.04	5.02	1340.68	Main-flush
200.10	5.04	5.02	1351.92	Main-flush
202.60	5.06	5.02	1369.16	Main-flush
210.11	5.06	5.02	1413.67	Main-flush
212.60	5.01	5.02	1773.30	Main-flush
217.61	2.94	16.00	1167.12	Main-flush
222.61	2.96	16.00	1164.45	Water
227.61	3.38	16.00	2046.17	Water
230.11	3.18	16.00	1746.03	Water
237.62	3.18	16.00	1739.23	Water
240.13	3.18	16.00	1735.09	Water
242.62	3.18	16.00	1727.95	Water
250.12	3.19	16.00	1714.14	Water
252.63	3.18	16.00	1711.00	Water
257.63	3.17	16.00	1703.72	Water
265.13	3.17	16.00	1684.91	Water
267.63	3.20	16.00	1725.77	Water
270.13	3.21	16.00	1718.64	Water
277.64	3.19	16.00	1710.83	Water
280.13	3.20	16.00	1707.69	Water
287.63	3.21	16.00	1699.27	Water
292.65	3.19	16.00	1698.09	Water

Table 5. Treatment record from Well#2 zone III.

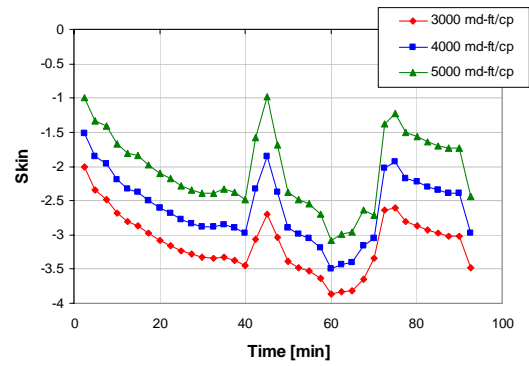


Figure 5 Skin factor sensitivity to kh/μ - Well#2 zone I.

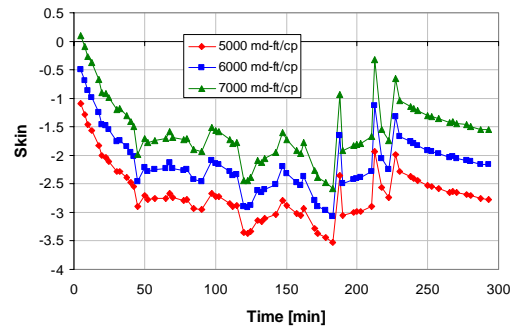


Figure 6 Skin factor sensitivity to kh/μ - Well#2 zone III.

In both analyses, variance in kh/μ shifts the skin evolution curves vertically but the overall trends remain the same. The normalized injectivity index of these analyses are plotted in figures 7 and 8.

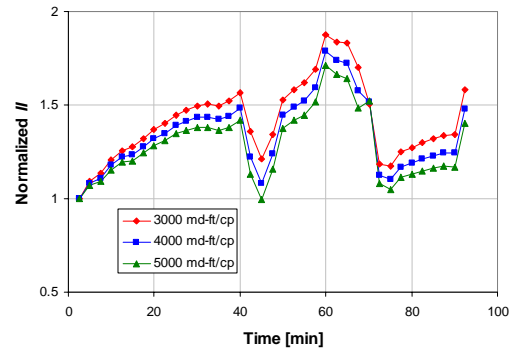


Figure 7 Normalized injectivity index sensitivity to kh/μ - Well#2 zone I

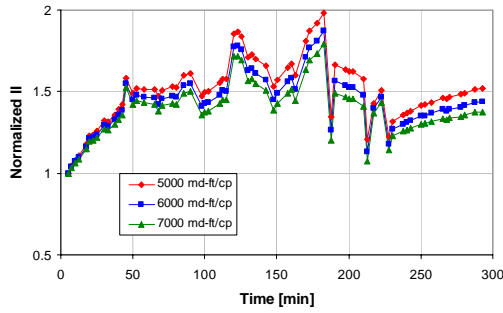


Figure 8 Normalized injectivity index sensitivity to kh/μ - Well#2 zone III

As can be seen in the figures, in any cases the analysis indicates injectivity improvement after the stimulation even though the magnitudes are different. Well #2 stimulation was very successful as indicated by the injectivity increase. Real-time analysis supports this result. Also, as opposed to Well #1 results, the skin factor did not increase much over the water flow.

SUMMARY AND CONCLUSIONS

We compared three existing real-time acid treatment evaluation methods. While Paccaloni's method predicts different behavior of skin evolution, the results projected by Prouvost and Economides, and Zhu and Hill are fairly close. We also conducted sensitivity studies with Zhu and Hill's method by applying several from the field.

From the study, we can draw the following conclusions:

1. Despite having unknown reservoir and fluid properties during the treatment which are known to affect the skin value, we found that they had limited impact on the qualitative behavior of the skin for treatments conducted at the Salak field.
2. In all analysis, skin factor shows an increasing trend during the water flow stage. This may be caused by precipitation or movement of plugging material further into fracture system.
3. Based on the observations, we recommend applying a higher rate for a longer duration in the water flow stage in order to try and push any damage away from the critical near wellbore region in future treatments.
4. For our data set, the Paccaloni method over-estimated the skin factor based on subsequent PLT and II test.

ACKNOWLEDGEMENTS

The authors wish to extend their sincerest gratitude to the management of Chevron Geothermal and Power for their kind permission to publish this work.

NOMENCLATURE

B	formation volume factor, RB/STB
c_t	total compressibility, 1/psi
h	formation thickness, ft
II	injectivity index, kph/psi
k	permeability, md
p_i	initial reservoir pressure, psi
p_r	reservoir pressure, psi
p_{th}	tubing head pressure, psi
p_{wf}	bottomhole pressure, psi
q	injection rate, bbl/day
r_e	reservoir radius, ft
r_b	acid bank radius, ft
s	skin factor, dimensionless
t	time, hour
Δp_h	hydrostatic head, psi
ϕ	porosity
μ	fluid viscosity, cp
ρ	density, lb/ft ³

REFERENCES

- Al-Dhafeeri, A.M., Engler, T.W., and Nasr-El-Din, H.A., "Application of Two Methods to Evaluate Matrix Acidizing Using Real-Time Skin Effect in Saudi Arabia," paper SPE 73703, presented at the 2002 SPE International Symposium and Exhibition on Formation Damage Control, Lafayette, LA, 20-21 February.
- Boonyapaluk, P., and Hareland, G., "Optimum Acid Volume Estimation Using Real-Time Skin Evaluation," paper SPE 36113, presented at the 1996 SPE Fourth Latin American and Caribbean Petroleum Engineering Conference in Port of Spain, 23-26 April.
- Earlougher, R.C.Jr: *Advances in Well Test Analysis, Monograph series*, SPE, Richardson, Texas (1977).
- Economides, M.J., Hill, A.D., and Ehlig-Economides, C.A.: *Petroleum Production Systems*, Prentice Hall Inc., New Jersey (1994).

Heard, S.R., Economides, M.J., and Ehlig-Economides, C.A., "Pressure and Rate Measurements to Validate Matrix Stimulation," paper SPE 19409, presented at the 1990 SPE Formation Damage Control Symposium, Lafayette, LA, February 22-23.

Mahajan, M. Pasikki, R., Gilmore, T., Riedel, K., and Steinback, S., "Successes Achieved in Acidizing of Geothermal Wells in Indonesia," paper SPE 100996, presented at the 2006 SPE Asia Pacific Oil & Gas Conference and Exhibition, Adelaide, Australia, 11-13 September.

Montgomery, C.T., Jan, Y-M., and Niemeyer, B.L., "Development of a Matrix-Acidizing Stimulation Treatment Evaluation and Recording System," *SPE Production and Facilities* (November, 1995) **219-224**.

Paccaloni, G., "New Method Proves Value of Stimulation Planning," *Oil & Gas Journal* (November, 1979) **155-60**.

Paccaloni, G., "Field History Verifies Control, Evaluation," *Oil & Gas Journal* (November, 1979) **161 - 165**.

Pasikki, R.G., and Gilmore, T.G., "Coiled Tubing Acid Stimulation: The Case of Awi 8-7 Production Well in Salak Geothermal Field, Indonesia," presented at the 31st Workshop on Geothermal Reservoir Engineering, Stanford, CA, 30, January - 1, February.

Prouvost, L.P., and Economides, M.J., "Applications of Real-Time Matrix Acidizing Evaluation Method," *SPE Production Engineering*, (November, 1989) **401-407**.

Zhu, D., and Hill, A.D., "Field Results Demonstrate Enhanced Matrix Acidizing Through Real-Time Monitoring," *SPE Production and Facilities* (November, 1998).

APPENDIX A

Downhole pressure measurement during acid treatment is often not feasible. Therefore, we need to convert tubing head pressure data into bottomhole by considering the hydrostatic head and frictional pressure loss. As accelerational pressure loss is negligible, the relationship between the tubing head and the bottomhole pressure can be written as

$$p_{wf} = p_{th} + \Delta p_h - \Delta p_f \quad (\text{A-1})$$

The hydrostatic head is calculated as

$$\Delta p_h = g \int_0^H \rho dz \quad (\text{A-2})$$

In field units,

$$\Delta p_h = \frac{1}{144} \int_0^H \rho dz \quad (\text{A-3})$$

where Δp_h is in psi, H is in ft, and ρ is in lb/ft³.

Frictional pressure loss can be written with the Fanning friction factor as

$$\Delta p_f = \frac{2f\rho v^2}{D} L \quad (\text{A-4})$$

where f is the fanning friction factor and defined as

$$f = \frac{2\tau_w}{\rho v^2} \quad (\text{A-5})$$

where τ_w is the shear stress at the pipe wall. For laminar flow, it can be solved analytically by applying boundary layer approximation as

$$f = \frac{16}{\text{Re}} \quad (\text{A-6})$$

where Re is the Reynolds number and is defined as

$$\text{Re} = \frac{\rho v D}{\mu} \quad (\text{A-7})$$

In the most applications, flow regime in pipe is turbulent and friction factor is obtained experimentally. The Moody frictional chart is the most commonly used and also equivalent explicit equation is available as (Economides *et al.*, 1993)

$$\frac{1}{\sqrt{f}} = -4 \log \left[\frac{\epsilon}{3.7065} - \frac{5.0452}{\text{Re}} \log \left\{ \frac{\epsilon^{1.1098}}{2.8257} + \left(\frac{7.149}{\text{Re}} \right)^{0.8981} \right\} \right] \quad (\text{A-8})$$